Analytica Chimica Acta 665 (2010) 98–104

Contents lists available at ScienceDirect

Analytica Chimica Acta

journal homepage: www.elsevier.com/locate/aca

An electrochemical immunosensor for carcinoembryonic antigen enhanced by self-assembled nanogold coatings on magnetic particles

Jianping Li[a,*], Huiling Gao[a], Zhiqiang Chen[a], Xiaoping Wei[a], Catherine F. Yang[b,**]

[a] College of Chemistry and Bioengineering, Guilin University of Technology, Guilin, 541004, China
[b] Department of Chemistry and Biochemistry, Rowan University, Glassboro, NJ 08028, USA

ARTICLE INFO

Article history:
Received 25 August 2009
Received in revised form 7 March 2010
Accepted 9 March 2010
Available online 19 March 2010

Keywords:
Magnetic particles
Carcinoembryonic antigen
Gold nanoparticle
Immunoassay
Layered assembly

ABSTRACT

A quick and reproducible electrochemical-based immunosensor technique, using magnetic core/shell particles that are coated with self-assembled multilayer of nanogold, has been developed. Magnetic particles that are structured from Au/Fe_3O_4 core–shells were prepared and aminated after a reaction between gold and thiourea, and additional multilayered coatings of gold nanoparticles were assembled on the surface of the core/shell particles. The carcinoembryonic antibody (anti-CEA) was immobilized on the modified magnetic particles, which were then attached on the surface of solid paraffin carbon paste electrode (SPCE) by an external magnetic field. This is an assembly of a novel immuno biosensor for carcinoembryonic antigen (CEA). The sensitivity and response features of this immunoassay are significantly affected by the surface area and the biological compatibility of the multilayered nanogold. The linear range for the detection of CEA was from 0.005 to 50 ng mL^{-1} and the limit of detection (LOD) was 0.001 ng mL^{-1}. The LOD is approximately 500 times more sensitive than that of the traditional enzyme-linked immunosorbent assay for CEA detection.

1. Introduction

Research on electrochemical immunoassay has attracted more attention from scientists in recent years. Such research can be easily conducted using simple electrochemical instruments that have excellent sensitivity and selectivity and the potential of miniaturization and automation [1]. Electrochemical immunoassay has been used to measure responses in potential, current, capacitance, and impedance during the immunoreaction between the antigens and the antibodies [2], among which the current-mode immunoassay is more favored for its high sensitivity. However, the immobilization of bioactivators on the surface of the transducer is the key to the fabrication of biosensors. When the immobilized materials are more active and the loading is larger, the electron transfer has lower resistance and the availability of regenerable sensor surface is the contributing factor [3]. One of the most effective platform technologies is the usage of magnetic nanoparticles as substrates for immobilizing bioactive materials, which can be separated by an external magnetic field. Magnetic nanoparticles have been widely used to develop biosensors through immobilizing enzymes [4–8], antibodies [9–14] and deoxyribonucleic acid on the nanoparticles [15,16].

Carcinoembryonic antigen (CEA) is commonly used as a clinical marker of tumors and elevated levels of CEA are correlated with cancer incidents [14]. The mass concentration of CEA in normal human serum is lower than 2.5 μg L^{-1}. The serological examination of CEA is important for the diagnoses of carcinoma of colon, lung cancer, cancer of pancreas, and stomach cancer as well as other Gland epithelial cancers.

A variety of immunoassays have been developed for the detection of CEA, such as radioimmunoassay, chemiluminescence immunoassay, enzyme-linked immunosorbent assay, fluoroimmunoassay, liposome immunoassay, and electrochemical immunoassay, etc. [17–21]. The electrochemical immunoassay exhibits unique effects in the related reports [22–35]. Recently, Yuan and co-workers reported a CEA immunoassay based on thionine-doped magnetic gold nanospheres as the label and horseradish peroxidase (HRP) as the enhancer [36] with a limit of detection (LOD) of 0.01 ng mL^{-1}. We have developed an amperometric CEA immunosensor based on covalent immobilization of the carcinoembryonic antibody (anti-CEA) on core/shell structured Au/Fe_3O_4 nanocomposites and the competitive immune reaction between CEA and HRP-labeled CEA with the anti-CEA [37]. In this biosensor, the surface of the Au/Fe_3O_4 magnetic nanoparticles was amino functionalized with thiourea, then the CEA antibody was covalently linked to the amino-modified particles with glutaraldehyde. The sensor showed a LOD of 0.57 ng mL^{-1}, which is not low enough for the detection of CEA due to the limited binding of CEA and HRP. In this study, we directly immobilized the anti-CEA on

* Corresponding author. Tel.: +86 773 2903121.
** Corresponding author. Tel.: +1 856 256 5455.
E-mail addresses: likianping@263.net (J. Li), yang@rowan.edu (C.F. Yang).

0003-2670/$ – see front matter © 2010 Elsevier B.V. All rights reserved.
doi:10.1016/j.aca.2010.03.020

the multilayered gold nanoparticles to develop a novel sensitive immunoassay. The Au/Fe_3O_4 magnetic composite nanoparticles were synthesized by the amination of the particles which were pretreated with thiourea. The multilayered gold nanoparticles were self-assembled on the surface of the composite magnetic particles and the anti-CEA was adsorbed and enriched on the multilayered Au nanoparticles, leading to the functionalized magnetic particles which were then attached on the surface of the solid paraffin carbon paste electrodes (SPCEs) by an external magnetic field. CEA is immuno-assayed using the competitive immune reactions of anti-CEA with CEA and Horseradish peroxidase labeled CEA antibody. The reported immunosensor, which is easy to prepare and use, exhibits high sensitivity and excellent selectivity. Furthermore the surface can be easily regenerated. It has been applied to the detection of CEA in human serum samples directly.

2. Experimental

2.1. Chemicals and equipments

The anti-CEA, CEA, and HRP-labeled CEA (HRP-CEA) were purchased from Bosai Biotechnology Ltd., Zhengzhou. The stock solution of CEA (10 μg L^{-1}) and anti-CEA (10 mg L^{-1}) were prepared in a 20 mmol L^{-1} phosphate buffer solution (PBS), and the stock solution of HRP-CEA (in PBS buffer) was diluted with the diluents in a volume ratio of 1:200. Thiourea was purchased from Tongguang Fine Chemicals, Beijing. Hydrochloroauric acid was purchased from Guoyao Group Chemical Reagents Co., Ltd., Shanghai. Bovine serum albumin (BSA) was purchased from Sigma Ltd. H_2O_2 (30%) was purchased from Guangzhou Chemical Reagents and the concentration was calibrated by a standard potassium permanganate solution. The 20 mmol L^{-1} PBS was prepared by mixing Na_2HPO_4 and KH_2PO_4 solutions. All the chemicals are of analytical grade.

Deionized water (>18.2 MΩ cm^{-1}) was used in all the experiments.

2.2. Preparation of core/shell Au/Fe_3O_4 nanoparticles

Fe_3O_4 nanoparticles were prepared with a reported procedure [6], where 4.64 g $FeCl_3{\cdot}6H_2O$ and 1.71 g $FeSO_4{\cdot}7H_2O$ were dissolved in 250 mL deionized water in the mole ratio of Fe^{2+}/Fe^{3+} = 1:2, and a 2 mL of 0.2 mol L^{-1} sulphuric acid was added to prevent the solution from the oxidation of Fe^{2+}. Ammonia (25%) was added till pH reached 9.0–9.5 and the solution was stirred for 30 min at room temperature. After amination the mixture was heated to 80 °C and kept for 30 min. A black suspension was produced and the mixture was sonicated for 10 min. The deposit was separated by a magnet, which was rinsed with hot water until the fluid became neutral. The Fe_3O_4 nanoparticles were then available in a flask for the preparation of Au/Fe_3O_4 nanoparticles.

A 0.229 g of sodium citrate was dissolved in 100 mL of deionised water, and the solution was heated to 99 °C under vigorous stirring, then a 1 mL of the prepared Fe_3O_4 suspension was added to the solution. Finally, a 5 mL of 10 mmol L^{-1} hydrochloroauric acid was dropped into the solution and kept reacting for 15 min. The water bath was removed and the suspension was continually stirred for 15 min. The solid was removed again by a magnet and rinsed with deionized water as the claret-red suspension was cooled down to the ambient temperature. An Au/Fe_3O_4 suspension was then prepared by dispersing the solid in 20 mL water which was kept at 4 °C. Gold nanoparticles were obtained by the reduction of hydrochloroauric acid with sodium citrate by using the same procedure, without addition of Fe_3O_4 suspension.

The Au/Fe_3O_4 particles and Au nanoparticles were collected by copper grids covered with carbon film from the diluted suspension of the as-prepared colloids. The collected particles were rinsed with deionised water and acetone, and were subsequently dried in ambient temperature. A H600 transmission electron microscope (Hitachi, Japan) was employed to assess the morphology of the nanoparticles at 200 kV. An energy dispersive X-ray spectroscopy (JEOL, Japan) was used to record the energy dispersive spectrum (EDS) of the magnetic particle. The X-ray photoelectron spectra (XPS) were taken using a Krators XSAM800 spectrometer equipped with a monochromatic MgK_α X-ray source (100 W, 12.5 KV). A TU-1901 dual-beam UV–vis spectrophotometer (Beijing Puxi Normal Instrument Ltd.) was also applied to characterize the colloids.

2.3. Preparation of immunosensors

A 0.5 mL aliquot of the aminated magnetic suspension was taken into a glass cell (Ø = 10 mm) with a strong rare earth magnet on the bottom. The solution was removed by the magnet, then a 0.5 mL of the as-prepared gold colloids was added to the reaction for 40 min to convert the gold nanoparticles on the Fe_3O_4 magnetic particles to a monolayer of gold. The monolayered gold/Fe_3O_4 particles were separated from colloid and then a 0.5 mL of 10 mmol L^{-1} thiourea solution was added back to the monolayered particles and reacted for 2 h. The magnetic particles were subsequently separated followed by adding gold colloid solution for 10 min. The procedure was repeated once again to obtain the multilayered nanogold [38]. The final production was dispersed in 0.5 mL PBS before use.

The solid paraffin carbon paste electrode (SPCE) (2 mm in diameter) was prepared according to the reported procedure [6]. The SPCE was polished on a piece of smooth paper, and was sonicated in the mixture of ethanol and nitrate acid (volume ratio = 1:1) for 3 min and was then rinsed with deionized water. A 20 μL aliquot of the magnetic suspension was dropped on the surface of the electrode, the electrode was then rinsed by PBS (pH 7.2). A 50 ng mL^{-1} of anti-CEA was dropped on the surface of the electrode. Then the electrode was rinsed with PBS again, and soaked in PBS at 4 °C prior to use. The preparation of anti-CEA/nano-Au/Au/Fe_3O_4 nanoparticles and the competitive immune reactions of anti-CEA on the nanoparticles were schematically shown in Scheme 1.

2.4. Electrochemical analysis

CHI660B electrochemistry workstation (Shanghai Chenhua Instrument Co., China) was adopted to control a three-electrode system where the as-prepared immunosensor acted as the work electrode and a platinum wire and a saturated calomel electrode (SCE) served as the counter and reference electrodes, respectively.

The anti-CEA immobilized immunosensor was initially reacted with 1% BSA at 37 °C for 15 min to isolate the non-specific adsorption. Then, it was incubated in a mixture of a given concentration of HRP-CEA and various concentrations of CEA at 37 °C. The cyclic voltammetry (CV) and differential pulse voltammetry (DPV) were carried out on the CHI660B electrochemical station where the scan range of CV was set between 0.8 and −0.6 V, and that for DPV was between 0.6 and −0.6 V with the pulse amplitude and width of 50 mV and 50 ms, respectively. The quantitative detection of CEA was carried out by DPV followed by a competitive immune reaction. The electrochemical analysis was performed by DPV in the PBS containing 1 mmol L^{-1} hydroquinone and 2 mmol L^{-1} of H_2O_2 at the temperature of 25 ± 0.5 °C.

3. Results and discussion

3.1. Characterization of core/shell Au/Fe_3O_4 magnetic nanoparticles

The TEM micrographs of the Au (a) and Au/Fe_3O_4 (b) nanoparticles are illustrated in Fig. 1. It is shown in Fig. 1a that the diameter of

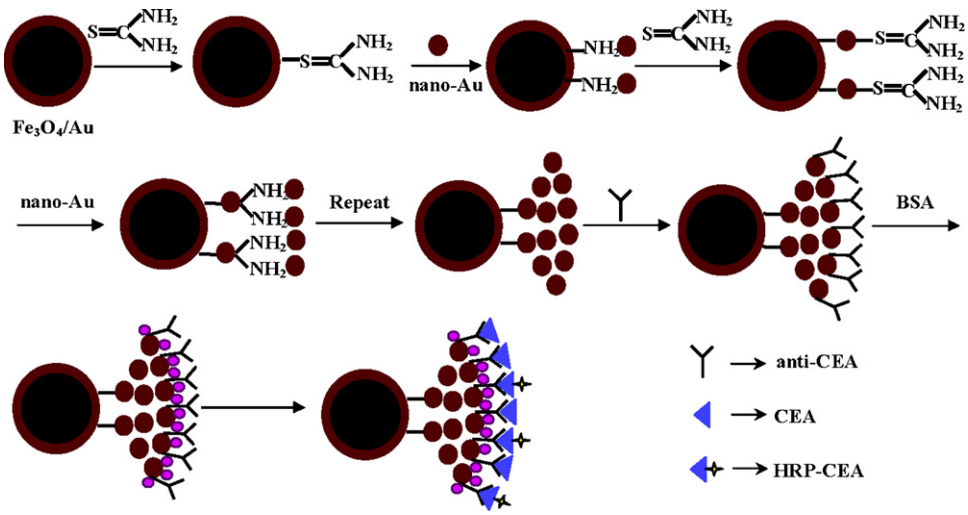

Scheme 1. Schematic diagram for the preparing of anti-CEA/nano-Au/Au/Fe_3O_4 nanoparticles and competitive immune reaction.

Au nanoparticles is narrowly distributed at 12.19 ± 0.69 nm (n = 45, 95%CI), whereas the Au/Fe_3O_4 composite nanoparticles have an average diameter of 28.91 ± 1.37 nm (n = 45, 95%CI), with no presence of integration.

The EDS spectrum of the Au/Fe_3O_4 nanoparticles showed the presence of Fe (25.61%, w/w), Au (47.88%, w/w) and O (8.29%, w/w), which suggested that the sheath consists of Au and Fe_3O_4.

The Au/Fe_3O_4 nanoparticles were also determined by X-ray photoelectron spectroscopy (XPS). Fig. 2(a) shows gold peaks including Au 4s, Au 4p, Au 4d, and Au 4f appeared on the surface of Fe_3O_4 particles. The Fe_3O_4 showed Fe 2p at 710–725 eV. The XPS of Au from the Au/Fe_3O_4 nanoparticles is shown in Fig. 2(b), in which the peak doublet of gold that appeared at 84.0 eV (Au $4f_{7/2}$) and 87.7 eV (Au $4f_{5/2}$) can be assigned to the Au^0.

The XPS results indicated that the surface of magnetic Fe_3O_4 has been coated with a shell of gold. The high intensity of Au peaks clearly indicated that the surface of the particle composites is mainly composed of gold.

Fig. 3 shows the UV–vis absorption curves of the Au nanoparticles, Fe_3O_4, and Au/Fe_3O_4 nanoparticle composites. Fe_3O_4 particles present no absorbance in the range from 300 to 800 nm. Gold nanoparticles exhibit the maximum absorbance at 520 nm, which is in agreement with Mie's theory [39]. The Au/Fe_3O_4 particles reach a maximum absorption peak at 533 nm, which is the characteristic absorbance of nanogold. The red-shifting in the nanoparticle composites is in agreement with their relatively larger diameters [40]. The peak in the nanoparticle composites is comparatively wider than that of the gold nanoparticles (marked as nanogold in Fig. 3). The TEM, EDS, and UV–vis spectroscopy results also indicated the formation of a coating of gold nanoparticles on the surface of the Fe_3O_4 nanoparticles.

3.2. Cyclic voltammograms of the immune reactions

The cyclic voltammograms of the SPCE with nanogold on the surface in PBS is shown in Fig. 4. The characteristic peak (curve a) for the oxidation of gold is clearly observed when the Au/Fe_3O_4 nanoparticles were attached on the surface of the SPCE by magnetic field. However, it disappeared when the Au/Fe_3O_4 nanoparticles reacted with thiourea and anti-CEA (curve b), suggesting the saturated assembly of thiourea *via* covalent coupling.

If an additional assembly operation for the Au/Fe_3O_4 modified electrode was carried out in the gold colloid, the gold oxide formation in the CV scans of the nano-Au/Au/Fe_3O_4/SPCE in PBS is apparently enhanced (curve c), indicating that more Au nanoparticles were loaded. Similarly, the gold oxide peak also decreased

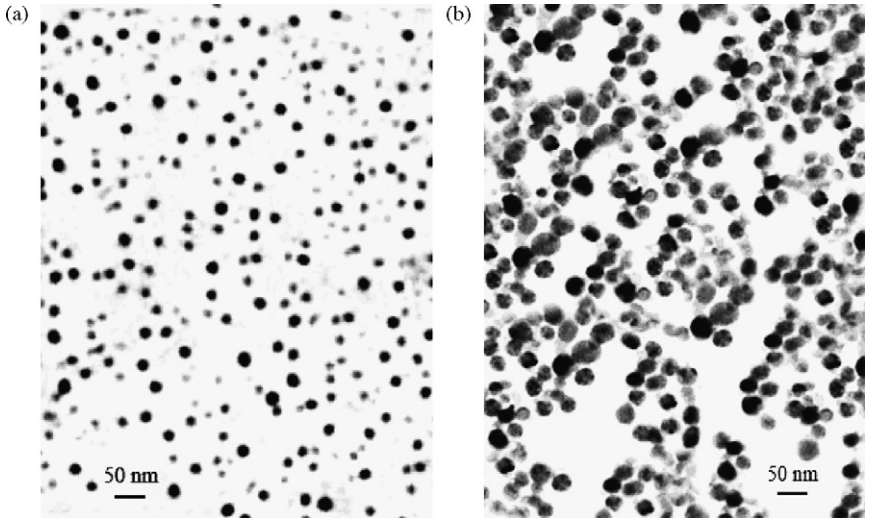

Fig. 1. TEM images of Au (a) and Au/Fe_3O_4 (b) nanoparticles.

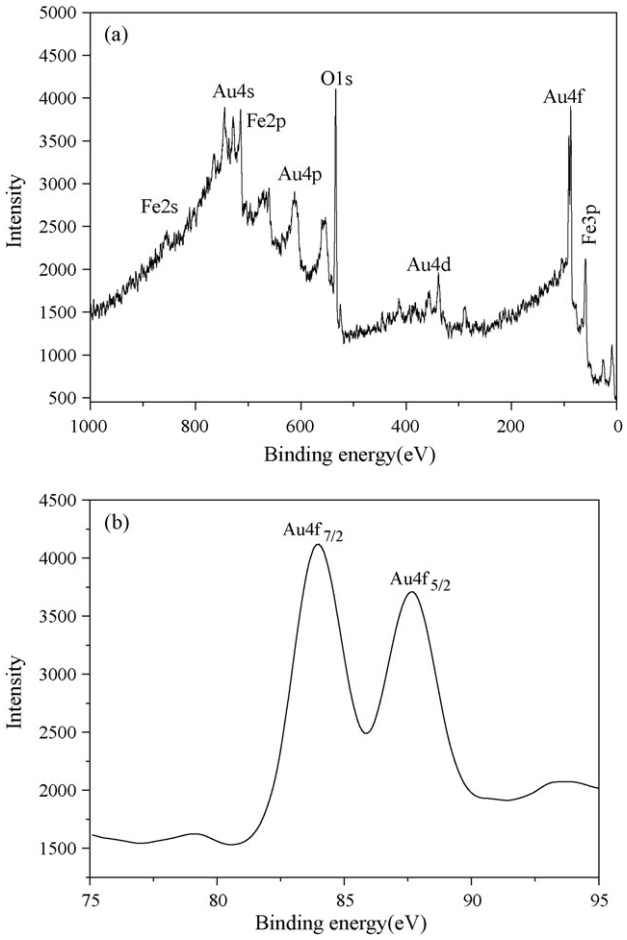

Fig. 2. XPS spectrum of the nano-Au/Au/Fe_3O_4 nanoparticles (a) and high resolution XPS spectrum of Au 4f (b).

when the nano-Au/Au/Fe_3O_4/SPCE electrode was reacted with 20 ng mL^{-1} anti-CEA solution.

3.3. DPV of the immunoassay

The detection of CEA was quantitatively determined by DPV, followed by the competitive immune reactions. The anti-CEA/Au/Fe_3O_4 and anti-CEA/nano-Au/Fe_3O_4 immobilized electrodes were placed in 1% BSA solution for 15 min to isolate the non-specific adsorption, and they were then incubated in a mixture of CEA and HRP-CEA in PBS (pH 7.4) at 37 °C for 20 min followed by the rinsing of the remained antigen by PBS. The DPV for the immunoassay was performed in a PBS (pH 7.4) containing 1 mmol L^{-1} hydroquinone and 2.0 mmol L^{-1} H_2O_2. The enzyme HRP catalyses the reaction between hydrogen peroxide and mediator hydroquinone (HQ), and the electrochemical biosensing is based on the voltammetric monitoring of the electro reduction of the oxidized mediator, benzoquinone (BQ). During the competitive assay, CEA (analyte) concentration is limited. The HRP-CEA competes with the unlabeled antigen CEA for binding to a limited amount of the corresponding anti-CEA on nano-Au/Fe_3O_4 electrode. The amount of HRP-CEA bound on anti-CEA/nano-Au/Fe_3O_4 electrode is inversely proportional to the amount of analyte antigen CEA, which leads to signal decreases as analyte concentration increases. The summarized results in Fig. 5 show that the recorded DPV currents are both decreased after the immobilized electrodes are incubated in the solution containing CEA and the current (Δi) changes with the concentration of CEA.

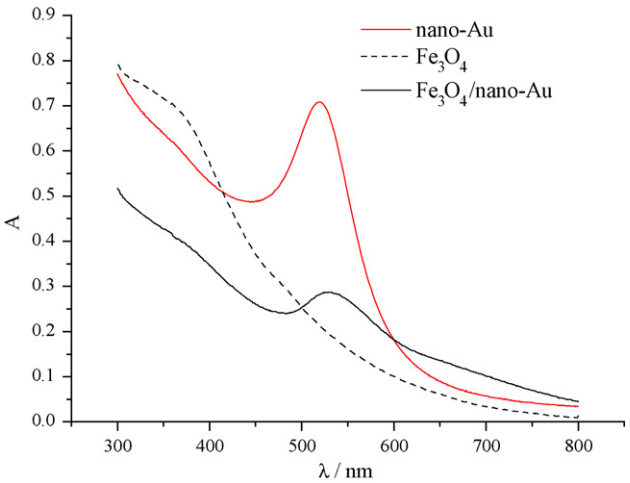

Fig. 3. UV–vis spectra of the nano-Au, Fe_3O_4 and Fe_3O_4/nano-Au nanoparticles.

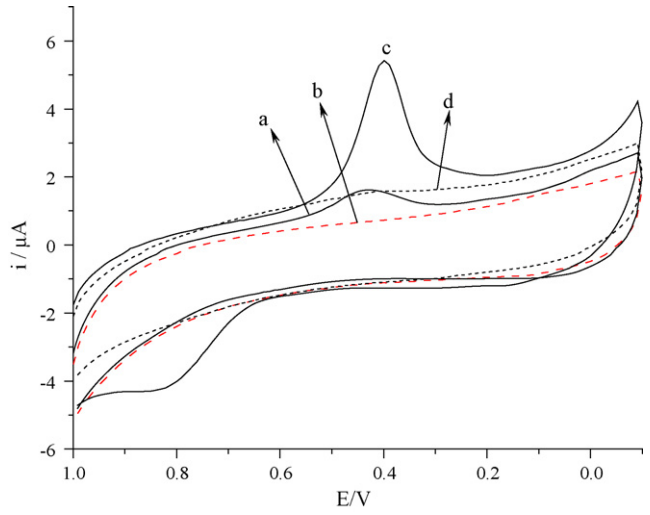

Fig. 4. CVs of the modified SPCEs in 0.02 mol L^{-1} PBS (pH 7.4) at a scan rate of 100 mV s^{-1}. (a) Au/Fe_3O_4/SPCE; (b) anti-CEA/Au/Fe_3O_4/SPCE, adsorbed for 40 min in a 20 ng mL^{-1} anti-CEA solution; (c) nano-Au/Au/Fe_3O_4/SPCE; (d) anti-CEA/nano-Au/Au/Fe_3O_4/SPCE, adsorbed for 40 min in a 20 ng mL^{-1} anti-CEA solution.

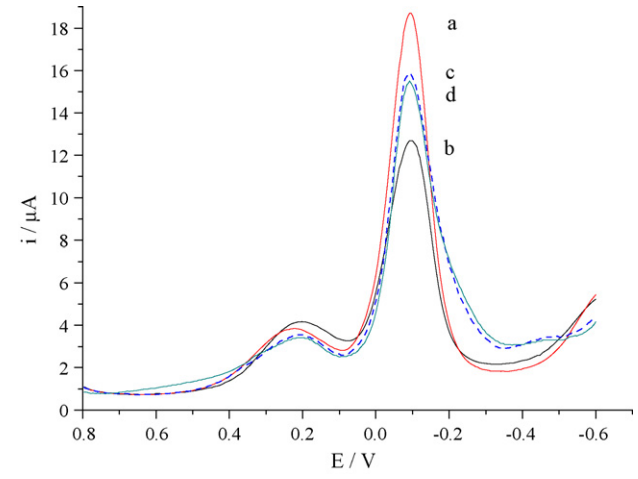

Fig. 5. DPV of the immunosensors in 1 mmol L^{-1} hydroquinone solution containing 2.0 mmol L^{-1} H_2O_2 in PBS (pH 7.4). (a) anti-CEA/nano-Au/Au/Fe_3O_4 SPCE, CEA: 0 ng mL^{-1}; (b) anti-CEA/nano-Au/Au/Fe_3O_4 SPCE, CEA: 0.5 ng mL^{-1}. (c) anti-CEA/Au/Fe_3O_4 SPCE, CEA: 0 ng mL^{-1}; (d) anti-CEA/Au/Fe_3O_4 SPCE, CEA: 0.5 ng mL^{-1}.

In contrast, the current difference of Δi for the anti-CEA/nano-Au/Fe_3O_4 electrode is ca. 25 times larger than that of anti-CEA/Au/Fe_3O_4. It is probably due to the large loading capacity and high immunoactivity of magnetic multilayer gold nanoparticles.

3.4. Optimization of parameters in the detection of CEA

3.4.1. The effects of buffer composition and pH value

The effects of the various buffer solutions and pH values on the immune reaction were examined, where a 0.02 mol L^{-1} phosphate buffer solution was selected for the immune reaction with the variation of pH from 6.0 to 8.5. The selection of this pH range is because the adsorption of nanogold on aminated magnetic particles and immuno binding reactions between CEA and its antibody are commonly occurred at nearly neutral solution. It was found that the current response Δi reaches the maximum when the immune reaction took place in pH 7.4 buffer solution; and therefore the experiments of immune reaction were selected in pH 7.4 PBS (0.02 mol L^{-1}).

3.4.2. The effects of immunoreaction incubation temperature and time

The combination of anti-CEA with CEA depends on the close interactions between such factors as hydrogen bonds, van der Waals forces, electrostatic forces, hydrophobic interaction forces [41]. There are numerous binding sites with the anti-CEA accessible to CEA. These intrinsic forces are generally believed to be maximal in physiological condition. The effect of the temperature and time of the immune reaction on the response of the immunoassay of 0.5 ng mL^{-1} CEA was studied. The current signals Δi of the immune reaction increased with temperature of electronic incubator in the range from 4 to 35 °C and reached its maximum at 37 °C, which was selected for the immune reaction between the immunosensor and the measured antigen. Further increase of temperature caused a decrease of the response.

The association between antibody and antigen requires certain time to form immunocomplexes. The immune reaction time was examined ranging from 10 to 50 min. It is evident that the response signals Δi steadily reach the maximum after the immune electrode when incubated in the analyte antigens for 20 min; which is, hence, selected as the parameter for the length of incubation time.

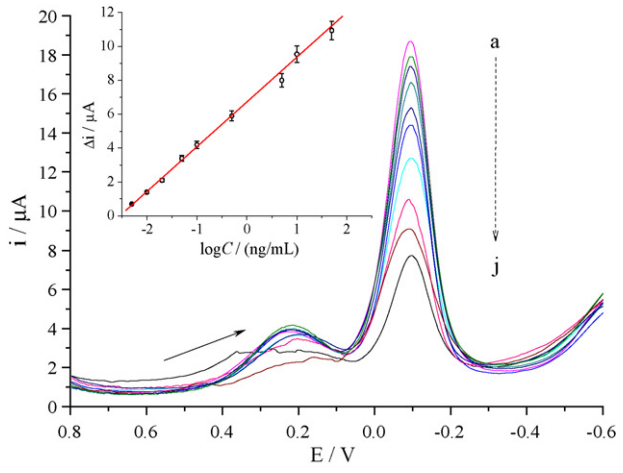

Fig. 6. The DPV scans of the proposed immunoassay incubated with 0 (a), 0.005 (b), 0.01 (c), 0.02 (d), 0.05 (e), 0.1 (f), 0.5 (g), 5 (h), 10 (i) and 50 ng mL^{-1} (j) CEA in solution containing 25 μL HRP-CEA in 1 mmol L^{-1} hydroquinone solution (pH 7.4) containing 2.0 mmol L^{-1} H_2O_2. Inset figure (logarithmic curve) is the calibration curve.

3.4.3. The amount of HRP-CEA

In the immune reaction, the analyte antigen CEA and a labeled derivative of the HRP-CEA compete for a limited number of antibody sites. After the competition has occurred, the conjugated HRP bound to the CEA has catalytic activity to the reduction of H_2O_2, owing to the electron mediator of hydroquinone. The generated catalytic current is inversely proportional to the concentration of CEA antigen in the sample.

In the case of maximization of the sensitivity of the immunoassay, the amount of HRP-CEA is fixed in the ratio of 1:1 to the amount of anti-CEA. During the assay, the stock solution of HRP-CEA with the diluent in a volume ratio of 1:200 was used. In order to test the expected amount of HRP-CEA in the experiments, the immunosensor was dipped in 1 mL of 20 mmol L^{-1} PBS (pH 7.4) containing various amounts of HRP-CEA, and the current response was recorded after incubation at 37 °C for 20 min in the stirring solution (100 rpm). The results indicate that the current Δi increases as 5–25 μL of HRP-CEA solution is added in the incubation solution, whereas more addition of HRP-CEA leads to a slight decrease of Δi, suggesting that the addition of 25 μL HRP-CEA has reached the maximum amount in 1 mL 20 mmol L^{-1} PBS for the reaction, and that the optimal amount of HRP-CEA in the mixed incubation solution is apparently chosen at 25 μL.

3.5. Detection of CEA

The anti-CEA immobilized electrode was placed in 1% BSA solution to isolate the non-specific adsorption for 15 min and was then moved into 1 mL PBS (pH 7.4) containing 25 μL HRP-CEA and various concentrations of CEA were incubated at 37 °C for 20 min with 100 rpm stirring. After washing off the uncombined antigen using PBS, the incubated immunosensor was placed in PBS (pH 7.4) containing 1 mmol L^{-1} hydroquinone and 2.0 mmol L^{-1} H_2O_2. DPV curves were recorded, and the CEA content in the solutions was quantitatively measured based on the decline of peak currents.

Fig. 6 illustrates the curves of CEA under the optimized condition and the standard curve as the DPV was applied on the immunoassay. The DPV current decreases with the concentration of CEA, where the linear regression is presented in the fitting between Δi and the logarithm of the concentrations of CEA in the range of 0.005–50 ng mL^{-1} as follows (shown in the inset figure):

$$\Delta i(\mu A) = 2.575 \log C(\text{ng mL}^{-1}) + 6.620$$

where the linear correlation coefficient $r = 0.9988$. Each value represents the mean value obtained by repeating the performances three times. The standard deviation is clearly indicated by error bars. The LOD is found as low as 0.001 ng mL^{-1} (S/N = 3), which is significantly lower than that of 0.57 ng mL^{-1} by the magnetic Au nanoparticle-based CEA immunosensor previously reported [37].

3.6. Reproducibility, selectivity and stability of the immunoassay

One of the most important factors for developing a practical immunosensor is its regeneration of the immunosensor surface. In this study the regeneration of the immunosensor surface was achieved simply and quickly by removing the magnet and rinsing out all of the magnetic substances on the electrode surface. The electrode is subsequently cleaned in 0.5 mol L^{-1} HCl and 50% ethanol mixture solution [11]. Compared with the regeneration method for breaking the antigen–antibody bond in strong acid solution [23], this developed method, based on the magnetic nanoparticles, is fairly convenient and applicative. The reproducibility for the fabrication was examined by five immunosensors prepared with different magnetic particles separately at the same SPCE in the measurement of 0.5 ng mL^{-1} CEA solutions. The

Table 1
The properties of this sensor compared with others reported.

Sensors	Linear response range ($ng\,mL^{-1}$)	Detection limit ($ng\,mL^{-1}$)	Refs
Anti-CEA/self-assembled thiourea monolayer/Au electrode	0.01–10	0.01	[24]
Anti-CEA/nano-Au/poly-o-aminophenol/Au electrode	0.5–20	0.1	[25]
Anti-CEA/colloid Au/SPCE (screen-printed carbon electrode	0.50–25	0.25	[26]
Anti-CEA/nano-Au/poly-sulfanilic acid/HRP/GCE	0.5–5.0		[27]
Anti-CEA/core-shell Fe_3O_4/SiO_2 nanoparticle	1.6–60	0.5	[28]
Anti-CEA/thionine/HRP/Au electrode	0.6–200	0.2	[29]
Anti-CEA/HRP/sol–gel, reagentless	0.5–120	0.4	[30]
Anti-CEA/nanogold/(3-mercaptopropyl)trimethoxysilane/nano-Fe_3O_4/carbon paste electrode	1.0–55	0.13	[31]
Anti-CEA/3-aminophenylboronic,11-mercaptoundecanoic acid/HRP/gold electrode	2.0–40.0	1.1	[32]
Anti-CEA/ferrocene carboxylic acid encapsulated liposomes/MWCNT screen-printed electrode	0.005–70	0.001	[33]
Anti-CEA/HRP-encapsulated nanogold hollow microspheres	2.5–1200.01–200	1.50.0015	[34]
Anti-CEA/nano-Au/Chit/NG/GCE	0.2–120.0	0.06	[35]
Anti-CEA/HRP/magnetic gold nanospheres	0.01–160	0.01	[36]
Anti-CEA/Au/Fe_3O_4 nanoparticle/SPCE	2–160	0.57	[37]
Anti-CEA/nano-Au particle/Au/Fe_3O_4 nanoparticle/SPCE	0.005–50	0.001	This sensor

response values Δi were obtained as $7.8 \pm 0.28\,\mu A$ with a relative standard deviation of 3.6%.

To evaluate the selectivity of the immunosensor, several components in human serum, which may cause interference with the detection, were examined. The results show that the response currents between Δi_0 (with no interferences) and Δi_1 (with interferences) produce the deviation of less than 5.0% once the immunosensor has been incubated in the $0.5\,ng\,mL^{-1}$ CEA solution coexisted with the interferences separately for 20 min. The interferences are listed as follows: AFP antigen ($100\,ng\,mL^{-1}$, 3.9%), CA125 antigen ($100\,ng\,mL^{-1}$, 4.4%), Hepatitis B surface antigen ($50\,ng\,mL^{-1}$, 4.9%), Hepatitis B core antigen ($80\,ng\,mL^{-1}$, 4.5%), α-Fetoprotein ($80\,ng\,mL^{-1}$, 5.0%), ascorbic acid ($20\,\mu g\,mL^{-1}$, 2.5%), L-glutamate ($10\,\mu g\,mL^{-1}$, 3.7%), urea ($0.40\,mg\,mL^{-1}$, 3.7%) as well as glucose ($1\,mg\,mL^{-1}$, 4.4%) respectively. The chosen concentrations are physiological relevant. The results indicate that the immunoassay exhibit a high selectivity and can effectively eliminate false-positives in practical application.

The stability of the magnetic colloid was also evaluated periodically by preparing immunosensors using the same amount of composite magnetic nanoparticles and DPV testing $5.0\,ng\,mL^{-1}$ CEA. It was tested 81 times in a period of 40 days by the method described in Section 2.4. The composite nanoparticles were stored in a sealed container and kept at 4 °C in the dark. It was found that the DPV current responses of Δi are 8.17 with a standard deviation of 0.455 for over 40 days, suggesting that the stability of the as-prepared immunoassay was kept well within 40 days. The current responses of Δi decreased 12% after 40 days. This indicates that the magnetic nanoparticles have acceptable stability.

The properties of this immunosensor compared with those described in some related reports are given in Table 1.

As can be seen, detection limit of the designed immunosensor was $0.001\,ng\,mL^{-1}$ indicated that it is one of the most sensitive CEA immunosensor. The analysis allows continuous test in almost 60 min for one sample, including biosensor preparing, incubation, washing, enzymatic reaction, determination procedures, and regeneration of sensor, which is shorter than that of the commercial ELISA (>4 h). Additionally, in contrast to other electrochemical immunosensor [24–27,28–35], the biosensor is easy to renew. The developed immunoassays may well provide a promising alternative tool for determining CEA in human serum in clinical laboratory.

Table 2
Determination results of CEA in serum samples by this immunosensor and chemiluminescence method.

Samples	Found ($ng\,mL^{-1}$) ($n=3$)	RSD (%)	Immuno-chemiluminescence ($ng\,mL^{-1}$)
1	21.5	4.37	20.6
2	23.0	2.22	22.5
3	40.21	1.45	40.8
4	5.29	1.73	5.2
5	73.2	0.55	72.8
6	14.16	3.21	13.72
7	50.23	1.30	50.89
8	83.7	1.95	82.1

4. Analytical applications

The immunoassay was used to analyze the serum samples of patients. Before determinations, proteins were separated from the serum samples by dialysis procedure using dialysis membrane (150 kDa). After dialysis, 100 μL retentate of serum sample was injected into 100 μL PBS ($20\,mmol\,L^{-1}$, pH 7.4). CEA was assayed by the method described in Section 2.4 and the results are compared to the clinical chemiluminescence method, which are sorted in Table 2. All the serum samples and the results of clinical analysis are kindly offered by Guilin Tumor Hospital. The measured immunoassay values have relative standard deviations ranging from −1.45% to 4.37%, to the clinical chemiluminescence method, showing an excellent agreement to the clinical method. The stated method in this paper is reproducible on the detection of CEA in human serum samples.

5. Conclusions

The multilayered coating of gold nanoparticles on the magnetic Au/Fe_3O_4 composites increased the specific surface area which increased the loading of immune reagents, i.e. CEA antibodies, and thus improved the efficiency of electron transfer. The improved electrochemical immunoassay exhibits high sensitivity, excellent stability, and a wide linear range for the detection of CEA. It is 100–1000 times more sensitive than that of ELISA. Furthermore, it is easy to prepare and is regenerable with low cost and short time. In conclusion, this novel electrochemical immunoassay technique is expected to be an effective clinical tool for fast and reliable tumor diagnosis.

Acknowledgements

The authors gratefully acknowledge the financial support from the National Science Foundation of China (no. 20665003), the Key Project of Science and Technology of the Ministry of Education of China (no. 207087), the Natural Science Foundation of Guangxi Province (no. 0728214) and the Innovation Project of Guangxi Graduate Education (no. 2007105960703M11).

References

[1] L.X. Tiefenauer, S. Kossek, C. Padeste, P. Thiébaud, Biosens. Bioelectron. 12 (1997) 213–223.
[2] P.D. Patel, Trends Anal. Chem. 21 (2002) 96–115.
[3] S. Zhang, G. Wright, Y. Yang, Biosens. Bioelectron. 15 (2000) 273–282.
[4] L.M. Rossi, A.D. Quach, Z. Rosenzweig, Anal. Bioanal. Chem. 380 (2004) 606–613.
[5] S. Qu, J. Wang, J. Kong, P. Yang, G. Chen, Talanta 71 (2007) 1096–1102.
[6] J. Li, X. Chen, Acta Chim. Sinica 66 (2008) 84–90.
[7] Y. Yuan, J. Li, Chin. J. Anal. Chem. 35 (2007) 1078–1082.
[8] J. Li, X. Wei, Y. Yuan, Sens. Actuators B: Chem. 139 (2009) 400–406.
[9] J.L. Gong, Y. Liang, Y. Huang, J.W. Chen, J.H. Jiang, G.L. Shen, R.Q. Yu, Biosens. Bioelectron. 22 (2007) 1501–1507.
[10] Z.M. Liu, H.F. Yang, Y.F. Li, Y.L. Liu, G.L. Shen, R.Q. Yu, Sens. Actuators B: Chem. 113 (2006) 956–962.
[11] J. Li, H. Gao, Electroanalysis 20 (2008) 881–887.
[12] H. Gao, J. Li, Chin. J. Anal. Chem. 36 (2008) 1614–1618.
[13] S. Centi, S. Laschi, M. Mascini, Talanta 73 (2007) 394–399.
[14] G. Messina, S. Tombelli, I. Palchetti, M. Mascini, Biosens. Bioelectron. 23 (2008) 1602–1609.
[15] G.K. Kouassi, J. Irudayaraj, Anal. Chem. 78 (2006) 3234–3241.
[16] J. Li, W. Zhu, H. Wang, Anal. Lett. 42 (2009) 366–380.
[17] M. Cioffi, M.T. Vietri, P. Gazzerro, Lung Cancer 33 (2001) 163–169.
[18] J.C. Forest, J. Masse, A.A. Lane, Clin. Biochem. 31 (1998) 81–88.
[19] V.M. Mekler, S.M. Bystryak, Anal. Chim. Acta 264 (1992) 359–363.
[20] K. Matsumoto, J.L. Yuan, G.L. Wang, H. Kimura, Anal. Biochem. 276 (1999) 81–87.
[21] M. Haga, S. Hoshino, H. Okada, N. Hazemoto, Chem. Pharm. Bull. 38 (1990) 252–254.
[22] D. Tang, R. Yuan, Y. Chai, Clin. Chem. 53 (2007) 1323–1329.
[23] J. Chen, G. Zou, X. Zhang, W. Jin, Electrochem. Commun. 11 (2009) 1457–1459.
[24] W. Limbut, P. Kanatharana, B. Mattiasson, P. Asawatreratanakul, P. Thavarungkul, Anal. Chim. Acta 561 (2006) 55–61.
[25] H. Tang, J. Chen, L. Nie, Y. Kuang, S. Yao, Biosens. Bioelectron. 22 (2007) 1061–1067.
[26] J. Wu, J. Tang, Z. Dai, F. Yan, H. Ju, E.N. Murr, Biosens. Bioelectron. 22 (2006) 102–108.
[27] X. Li, R. Yuan, Y. Chai, L. Zhang, Y. Zhuo, Y. Zhang, J. Biotechnol. 123 (2006) 356–366.
[28] J. Pan, Q. Yang, Anal. Bioanal. Chem. 388 (2007) 279–286.
[29] Z. Dai, J. Chen, F. Yan, H. Ju, Cancer Detect. Prev. 29 (2005) 233–240.
[30] F. Tan, F. Yan, H. Ju, Electrochem. Commun. 8 (2006) 1835–1839.
[31] D. Tang, B. Xia, Microchim. Acta 163 (2008) 41–48.
[32] X. Zhang, Y. Wu, Y. Tu, S. Liu, Analyst 133 (2008) 485–492.
[33] S. Viswanathan, C. Rani, A.V. Anand, J.A. Ho, Biosens. Bioelectron. 24 (2009) 1984–1989.
[34] D. Tang, J. Ren, Anal. Chem. 80 (2008) 8064–8070.
[35] X. He, R. Yuan, Y. Chai, Y. Shi, J. Biochem. Biophys. Methods 70 (2008) 823–829.
[36] D. Tang, R. Yuan, Y. Chai, Anal. Chem. 80 (2008) 1582–1588.
[37] J. Li, H. Gao, Z. Xiong, Chem. J. Chin. Univ. 29 (2008) 2149–2154.
[38] H. Huang, X. Yang, Colloids Surf. A 226 (2003) 77–86.
[39] G. Mie, Ann. Phys. 25 (1908) 377–445.
[40] U. Kreibig, L. Genzel, Surf. Sci. 156 (1985) 678–700.
[41] P.M. Colman, Structure of antibody-antigen complexes: implications for immune recognition, in: H.G. Kunkel, F.J. Dixon (Eds.), Advances in immunology, vol. 43, Academic Press, New York, 1988, pp. 99–132.